MODEL-BASED MULTIPLE FAULT DETECTION AND ISOLATION FOR NONLINEAR SYSTEMS

Ivan Castillo, and Thomas F. Edgar
The University of Texas at Austin
Austin, TX 78712

David Hill
Chemstations
Houston, TX 77009

Abstract

A model-based detection and isolation (FDI) system based on nonlinear state estimation and high filtering conditions is proposed. A better understanding of the residual trends, calculated from the difference between measurements and the extended Kalman filter (EKF) estimates, can be obtained when a fault occurs by developing a model that is able to predict the behavior of the residuals. This residuals model is utilized as the basis for detection and isolation of multiple faults, having the advantage of distinguishing single and multiple faults from a diverse array of possible faults, a common occurrence in complex processes. The proposed approach is validated using a CSTR, which is simulated using unit operation software CHEMCAD.

Keywords

Nonlinear fault detection and isolation (FDI), Residuals modeling, FDI of Multiple faults, CHEMCAD CSTR simulations.

Introduction

Nonlinear model-based FDI systems (Venkatasubramanian et al., 2003 and Castillo et al., 2010) use dynamic models that are physically-based or empirically-defined. A typical model-based approach utilizes nonlinear state estimators and the concept of analytical redundancy, where residuals are derived by calculating the difference between the actual outputs of the monitored system with the outputs obtained from a mathematical model and the state estimator. To detect faults, the residuals are evaluated by using either threshold values or statistical decisions. To isolate faults, a signature matrix can be defined in which residuals that fall outside of the threshold values are matched with different faults that could occur in the system. Parameter estimation is another alternative for isolation (Isermann, 2005), whereby variations of parameters of the nonlinear model, from their nominal operation values, are associated with different faults. The latter isolation technique is known as a parametric approach. The disadvantage of these model-based approaches lies in the isolation of multiple faults in which distinguishing one from another becomes a formidable task. In this paper, multiple fault cases are analyzed when different kinds of faults (such as sensor, actuator or process faults) are included under a restrictive amount of available measurements. With this restriction, there is no guarantee of successful identification, except for extracting major information from the residuals. Therefore, the main contribution of this paper is to develop an FDI system based on developing a high fidelity model that is able to predict and understand residual dynamics in the event fault occurs in a nonlinear system.

The proposed architecture, based on residuals modeling to detect and isolate faults, is illustrated in Figure 1. The right portion of Figure 1 illustrates how the FDI system is designed. A state estimator, which has different characteristics than the one used for control purposes (shown on the left hand side), is utilized to generate the residuals. These residual trends Res_k can be

predicted using the residuals model block at each time step. Additionally, using both the residuals Res_k and predicted residual trends r_k, the mechanism of detection is designed whereby the detection of the fault is performed at each time step. Once a fault is detected, the residuals model and the residual signals are utilized to isolate the faults at each time step. At the output of this isolation block, different modes are generated, such as $Fault_{i_k}$ or False Alarm. These four components (the state estimator, residuals model, the detection and isolation mechanisms) are briefly presented in the next section.

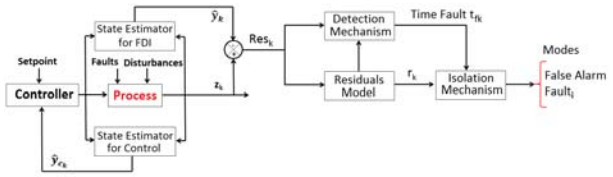

Figure 1: Fault Detection and Isolation (FDI) System

This paper is comprised of six sections. Section 2 formulates the dynamic residuals model as well as the FDI mechanism. Next, Section 3 presents the CSTR system that is simulated by using CHEMCAD in which control loops and faults are created using this unit operation software. The multiple fault case is presented in Section 4, followed by the validation of the residuals modeling approach in Section 5. Finally, closing remarks are presented in Section 6.

FDI Mechanism Based on Residuals Modeling

The residuals model is derived by considering the following assumptions: (1) the process is formulated as a nonlinear stochastic differential equation shown in Eqs. (1) and (2); (2) the nonlinear system is observable; (3) the effect of the noises *w* and *v* is considered, even though these vectors are unknown; and (4) a state estimator is needed. Then, the extended Kalman filter (EKF) will be utilized for the formulation of this function.

$$x_k = f(x_{k-1}, u_{k-1}, w_{k-1}) \quad (1)$$

$$y_k = h(x_k, v_k) \quad (2)$$

where: $x \in \Re^n$ is the vector of state variables, $u \in \Re^m$ is the vector of system inputs, $y \in \Re^p$ is the vector of system outputs, $f(\cdot)$ is the nonlinear state equation function, $h(\cdot)$ is the nonlinear output function, *w* and *v* are gaussian white noises with covariance matrices Q_k and R_k respectively. These covariances satisfy the following conditions: $E(w_k\, w_j^T) = Q_k \delta_{k-j}$, $E(v_k\, v_j^T) = R_k \delta_{k-j}$, and $E(v_k\, w_j^T) = 0$.

The extended Kalman filter (EKF), which is an important component to determine the residuals model, is a widely used algorithm for nonlinear state estimation (Simon, 2006). The EKF linearizes the model about the current estimated state. The prediction of the state variables $\hat{x} \in \Re^n$ is obtained using Eq. (3), which is in terms of the Kalman gain K_k and the measurement vector $z_k \in \Re^p$,

$$\hat{x}_k = f(\hat{x}_{k-1}, u_{k-1}, 0) + K_k\left[z_k - h\left(f(\hat{x}_{k-1}, u_{k-1}, 0), 0\right)\right] \quad (3)$$

note that depending upon the value of the Kalman gain which is in terms of the noise covariances. Additional filtering results from giving more priority to the model predictions (first term on the right hand side of Eq. (3)). Therefore, small values of the Kalman gain can be obtained when the norm of the ratio R_k / Q_k is more than 1.

The residuals Res_k, Eq. (4), are calculated from the difference between measurement vector $z_k \in \Re^p$ and the EKF outputs' estimates $\hat{y}_k = h(\hat{x}_k, 0) \in \Re^p$. The predicted residuals $r_k \in \Re^p$ refer to the values obtained from the residuals model, given by Eq. (5),

$$Res_k = z_k - \hat{y}_k \approx r_k \quad (4)$$

$$r_k = \alpha_k + H_k^*(I - K_k H_k)\eta - H_k^* K_k \gamma + H_k^*(I - K_k H_k) A_k \phi_{k-1}\left[r_{k-1} - \alpha\right] \quad (5)$$

where: the vectors α, η and γ result from noise effects and errors in the modeling. $H_k \in \Re^{pxn}$ and $H_k^* \in \Re^{pxn}$ are the Jacobian matrices given by Eqs. (6) and (7) respectively:

$$H_{k_{[i,j]}} = \left.\frac{\partial h_{[i]}}{\partial x_{[j]}}\right|_{\left(x_k^- = f(\hat{x}_{k-1}, u_{k-1}, 0), 0\right)} \quad (6)$$

$$H^*_{k_{[i,j]}} = \left.\frac{\partial h_{[i]}}{\partial x_{[j]}}\right|_{(\hat{x}_k, 0)} \quad (7)$$

ϕ_k for the non-square case, which applies for the case study, is calculated using Eq. (8).

$$\phi_{k-1} = \begin{cases} H_{k-1}^{*T}\left(H_{k-1}^* H_{k-1}^{*T}\right)^{-1}, & p < n \\ \left(H_{k-1}^* H_{k-1}^{*T}\right)^{-1} H_{k-1}^{*T}, & p > n \end{cases} \quad (8)$$

Note that the residuals model, given by Eq. (5), is in terms of the Kalman gain K_k which permits to control less or more filtering in the state estimations. Under conditions of normal operation and low filtering, the magnitude of the residuals is close to zero. However, a larger magnitude of the residuals can be obtained when more filtering is designed in the Kalman filter, making it possible to analyze its dynamic for purposes of detection and isolation of faults.

The detection of a fault is evaluated in the space of the residuals, whereby multiple spaces can be generated providing redundancy and increasing sensitivity for detection. Three different kinds of residual spaces can be generated: (1) spaces that include residuals (Eq. (4))

versus predicted residuals (Eq. (5)); (2) residual spaces that are comprised of two different residuals obtained from Eq. (4); and (3) residual spaces that are derived from the predictive residuals formulated in Eq. (5). These residual trends can be enclosed by defining a trajectory that best represents the normal operating behavior of the system. Elliptical trajectories are defined for each residual space. Therefore, a fault is detected once any of these residual trajectories surpass the elliptical trajectories in any residual space.

Three steps are considered to isolate faults. First, multiple modes are defined in the isolation system: (1) a false alarm mode; (2) different single and multiple fault modes f_i that include sensor, actuator or process faults; and (3) unknown fault mode. Second, for each of the single and multiple fault cases f_i, parameters of the residuals model Eq. (5) are associated with each fault mode and defined as P_{f_i}. Note that the parameters that consider the effect of noise and model mismatch, such as η, γ and α, can be considered in addition to the parameters of the nonlinear model. Third, the objective function of Eq. (9) is utilized to calculate the parameters P_{f_i} of each single and multiple fault case at each time step,

$$\begin{aligned} J_k &= \min_{P_{fik}} \Delta_{f_{ik}}^T W \Delta_{f_{ik}} \\ lb &\le P_{f_{ik}} \le ub \end{aligned} \tag{9}$$

where the matrix $W \in \Re^{pxp}$ is a weighting constant. The lower and upper bounds of the parameters to be estimated are given by *lb* and *ub* respectively. The function $\Delta_{f_{ik}}$, which is in terms of the parameters P_{f_i} associated with each fault case f_i, is given by Eq. (10). Once a fault is detected, every $\Delta_{f_{ik}}$ is calculated. Then, a false alarm is diagnosed when Δ_{NO_k}, which is obtained by calculating the difference between the values of the predicted residuals and residual values in normal operation, is smaller than all the $\Delta_{f_{ik}}$ cases considered. Otherwise, the fault f_i is identified by comparing the multiple $\Delta_{f_{ik}}$ against each other. In the case there are inconsistent comparisons, an unknown fault is diagnosed.

$$\Delta_{f_{ik}} = \left| r_k\left(P_{f_{ik}}\right) \right| - \left| Res_k \right| \tag{10}$$

Non-isothermal Chemical Reactor

The hydrolysis of propylene oxide to propylene glycol (Bakosova et al., 2009), where the reaction is defined by Eq. (11), is simulated using CHEMCAD through a nonisothermal CSTR reactor.

$$C_3H_6O + H_2O \rightarrow C_3H_8O_2 \tag{11}$$

Figure 2 shows the P&ID of the system. The reactor has two inputs: (1) the flow of propylene oxide $F_{PO}\left[m^3/\min\right]$ which is represented by feed stream 1; and (2) the flow of water $F_W\left[m^3/\min\right]$, given by feed stream 7, which is proportional to the opening of the control valve given by unit operation number 5. The output $F_r\left[m^3/\min\right]$ of the reactor is given by product stream 6. The jacket of the reactor is fed with cooling water flow $F_c\left[m^3/\min\right]$, given by feed stream 5, which is proportional to the opening of the control valve denoted by unit operation number 3.

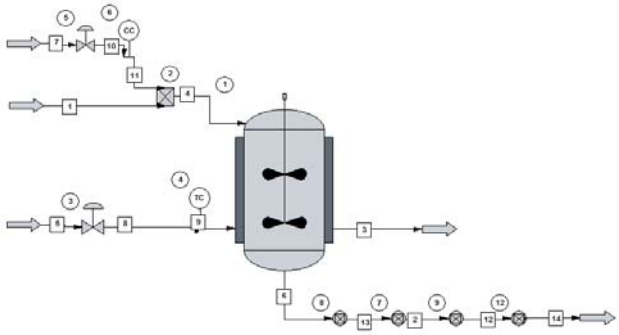

Figure 2: CSTR P&ID Diagram Using CHEMCAD

The dependence of a reaction rate constant on the temperature is described by the Arrhenius equation, given by Eq. (12) and the reaction kinetics, which is in terms of the concentration of the propylene oxide $C_{PO}\left[kmol/m^3\right]$ and water $C_W\left[kmol/m^3\right]$, and is of the second order, given by Eq. (13).

$$k = k_0 e^{-\frac{E}{RT_r}} \tag{12}$$

$$r = C_{PO} C_W k_0 e^{-\frac{E}{RT_r}} \tag{13}$$

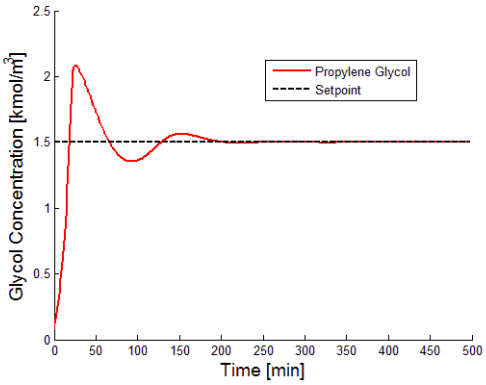

Figure 3: Concentration Propylene Glycol Control Loop Trajectory

Two PI controllers maintain the temperature of the reactor $T_r\left[^\circ K\right]$ and the concentration of the propylene glycol $C_{PG}\left[kmol/m^3\right]$ within a desired range. The temperature in the reactor is controlled by manipulating the jacket cooling flow, which is proportional to the

opening of the valve with unit operation number 3. On the other hand, the concentration of glycol is controlled by manipulating the water flow through the opening of the control valve with unit operation number 5. Figures 3 and 4 show the performance of the controllers whereby the black (dashed) lines correspond to the set point trajectories and the red (thin) lines represent the process variables.

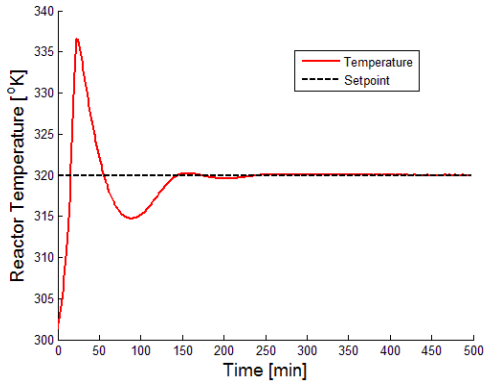

Figure 4: Reactor Temperature Control Loop Trajectory

Fault Case Scenario

The multiple fault case, simulated using CHEMCAD (Massey, 2002), is the combination of both sensor and actuator faults. The faults are simulated at t=250-400min. The sensor fault is created through inserting a constant bias in the reactor temperature sensor. This fault generates an instantaneous change in the reactor temperature and a fast response in the controller temperature, therefore causing changes in the temperature of the jacket.

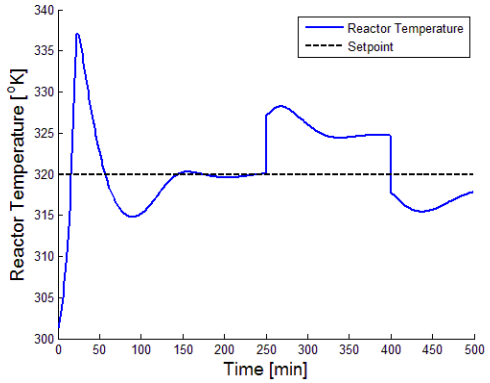

Figure 5: Reactor Temperature under Sensor and Actuator Fault

The actuator fault is created by modifying the coefficient of the control valve of the jacket. The flow of the cooling jacket decreases and creates an increment in the reactor and jacket temperatures. Figures 5 and 6 show the reactor and jacket temperature trajectories under these two faults. These trends are similar to the single sensor and actuator fault cases, making the task of isolation a formidable one.

Fault Detection and Isolation Results

The parameters of the residuals model, given by Eq. (5), are obtained and listed in Table 1. The elliptical trajectories are calculated from the normal operation data in which nine residual spaces were created. Figure 7 shows an example of the residual spaces created in normal operation.

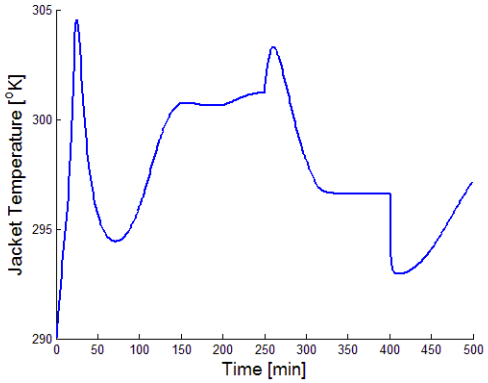

Figure 6: Jacket Temperature under Sensor and Actuator Fault

Table 1. Parameters of the Residuals Model

Parameters	CSTR
α	$\begin{bmatrix}1.52 & 2.85*10^{-5} & 8.43*10^{-7}\end{bmatrix}^T$
η	$\begin{bmatrix}0 & 0 & 8.52*10^{-4} & 0.29 & 0.12\end{bmatrix}^T$
γ	$\begin{bmatrix}1.63 & 6.72*10^{-6} & 5.27e^{-7}\end{bmatrix}^T$

Figure 8 shows the isolation results for the multiple fault case considered. The results are summarized in Table 2 in which good isolation results were obtained. During the first 30 seconds, some incorrect detection and isolation statements are generated. These errors are obtained because both the CSTR and the Kalman state estimator start at different initial conditions, consequently the magnitude of the residuals is big enough to generate these FDI errors, until the state estimator reaches convergence. Some false alarms are confirmed in the isolation statement given by the blue bars, the multiple fault is indicated by the cyan bar.

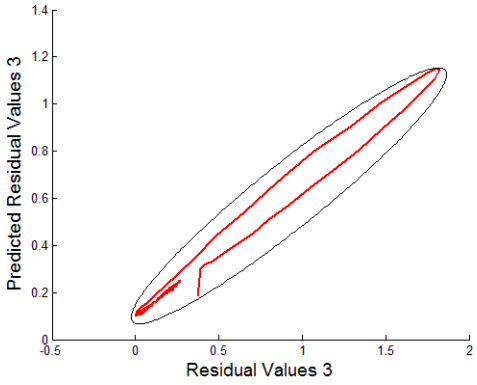

Figure 7: Residual Values 3 versus Predicted Residual Values 3

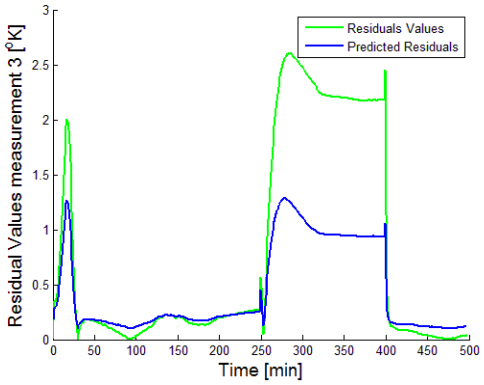

Figure 9: Residual Values and Predicted Residual Values versus Time

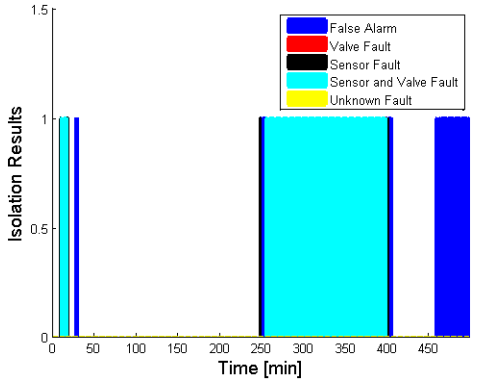

Figure 8: Isolation Results Sensor and Actuator (Valve) Fault

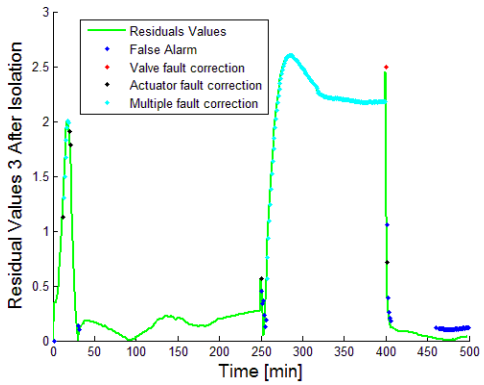

Figure 10: Residual Values and Predicted Residual Values versus Time After Isolation

Table 2. Fault Detection and Isolation Results CSTR Case Study

Criteria	Actuator-Sensor Fault
Total Number of Detections	207
Pct. of Correct Isolation of the Fault [%]	94.7
Pct. of Correct Detection [%]	72.9
Pct. of Correct Isolation of False Alarms [%]	80.4

To better understand how the isolation mechanism is performed, Fig. 9 shows the residuals trajectories for the multiple fault case before the fault is isolated. The green line corresponds to the residual values and the blue line illustrates the predicted residual values. Notice that the difference between the predicted residuals and the residual values, defined as $\Delta_{f_{ik}}$ in Eq. (10), is captured by the detection mechanism. Figure 10 shows the results after the parameter estimation is calculated, in which the faulty residual values are matched using the residuals model and the estimation of the parameters associated with each fault.

Conclusions

A model that predicts the residuals dynamic behavior is formulated in this paper and used with the purpose of fault detection and isolation. The approach is based on a nonlinear state estimator and the estimation goals are based on performing high filtering over the measurements. In this way, the magnitude of the residuals will be important enough to be analyzed. In using this residuals model, a better understanding regarding the residual trends, when a fault occurs, can be studied and further utilized to isolate faults efficiently. The detection is performed by analyzing the residual trends of both residuals signals and predicted residuals. Multiple fault modes are defined and validated through parameter estimation for the isolation mechanism. The approach has the advantage of verifying false alarms.

Having a restricted number of measurements available makes the objectives of detection and isolation a formidable task. However, it has been demonstrated that the residuals modeling based approach can deal with this restriction. A nonlinear process, simulated using CHEMCAD, was utilized to successfully validate the proposed approach, showing acceptable performance under both closed-loop and open-loop situations. These

results serve as important evidence to extend the FDI formulation to other nonlinear applications.

Acknowledgments

The authors want to thank the Process Science & Technology Center (PSTC) at the University of Texas at Austin and the Roberto Rocca Foundation for the support of this project.

Appendix: CSTR Model Parameters

The CSTR simulation parameters are:

The preexponential factor or frequency factor, $k_0\left[\min^{-1}\right]$, is $2.4067*10^{11}$; which is utilized in the Arrhenius equation (given by Eq. 11).

The activation energy, $E\left[kJ/kmol\right]$, is 84666.3

The universal gas constant, $R\left[kJ/kmol-^{\circ}K\right]$, is 8.314

$k\left[\min^{-1}\right]$, defined in Eq. 11, is the specific reaction rate.

$T_r\left[^{\circ}K\right]$ is the reactor temperature.

$r\left[kmol/\min - m^3\right]$, defined by Eq. 12, is the rate of consumption of reactants.

The volume of the reactor, $V_r\left[m^3\right]$, is 3.

Three molar concentrations are considered: (1) concentration of the propylene oxide, C_{PO}; (2) concentration of the water, C_W; and (3) the concentration of the propylene glycol, C_{PG}.

$F_r\left[m^3/\min\right]$ is the inlet/outlet flow rate of the reactor and represented by feed stream 4 (shown in Fig. 1).

The propylene oxide flow rate, $F_{PO}\left[m^3/\min\right]$, is held constant at approximately 0.012. The water flow, $F_W\left[m^3/\min\right]$, is proportional to the opening of the control valve denoted by unit operation 5. The flow rate through the control valve is given by:

$$F_W = \frac{U_{cr}}{100}\left[1-\frac{1}{Rang}\right]k_{cv5}\sqrt{\Delta P}$$

where the rangeability, $Rang$, is 10. The valve position, $U_{cr}\left[\%\right]$, is obtained from the propylene glycol controller. The differential pressure of the valve, $\Delta P\left[\text{bar}\right]$, is assumed constant at 0.1. The coefficient of the valve, k_{cv5}, is 0.721.

Similarly, the coolant flow, $F_c\left[m^3/\min\right]$, is proportional to the opening of the control valve, denoted by unit operation 3, and calculated using the following equation:

$$F_c = \frac{U_{cc}}{100}\left[1-\frac{1}{Rang}\right]k_{cv3}\sqrt{\Delta P}$$

where the valve position, $U_{cc}\left[\%\right]$, is obtained from the reactor temperature controller. The coefficient of the valve, k_{cv3}, is 1.152.

References

Bakoov, M., Puna D., Dostl P., and Zvack J. (2009). Robust stabilization of a chemical reactor. *Chemical Papers*, 63(5), 527-536.

Castillo, I., Edgar, T.F., and Dunia R. (2010). Nonlinear model-based fault detection with fuzzy set fault isolation. *IECON 2010 - 36th Annual Conference on IEEE Industrial Electronics Society*, Nov., 174-179.

Isermann, R. (2005). Model-based fault-detection and diagnosis - status and applications. *Annual Reviews in Control*, 29(1), 71-85.

Massey, N. (2002). Incorporating Reality Into Process Simulation. http://www.chemstations.com/content/documents/Technical_Articles/nmreality.pdf

Simon, D. (2006). Optimal state estimation: Kalman, H infinite and nonlinear approaches. *John Wiley & Sons*.

Venkatasubramanian V., Rengaswamy R., Yin K., and Kavuri S. (2003). A review of process fault detection and diagnosis: Part I: Quantitative model-based methods. *Computers & Chemical Engineering*, 27(3), 293-311.